Article

Quantitative and Qualitative Analysis of Aircraft Round-Trip Times Using Phase Type Distributions

Srinivas R. Chakravarthy

Departments of Industrial and Manufacturing Engineering & Mathematics, Kettering University, Flint, MI 48504, USA; schakrav@kettering.edu; Tel.: +1-810-610-8391

Abstract: One of the major issues facing commercial airlines is the time that it takes to board passengers. Further, most airlines wish to increase the number of trips that an aircraft can make between two or more cities. Thus, reducing the overall boarding times by a few minutes will have a significant impact on the number of trips made by an aircraft, as well as enabling improvements in key measures such as the median and 75th and 95th percentiles. Looking at such measures other than the mean is critical as it is well known that the mean can under- or overestimate the performance of any model. While there is considerable literature on the study of strategies to decrease boarding times, the same cannot be said about the study of the boarding time given a particular strategy for boarding. Thus, the focus of this paper is to study analytically (using suitable stochastic models) and numerically the impact of reducing the average time on the key measures to help the system to plan accordingly. This is achieved using a well-known probability distribution, namely the phase type distribution, to model various events involved in the boarding process. Illustrative numerical results show a reduction in the percentile values when the average boarding times are decreased. Understanding the percentiles of the boarding times, as opposed to relying only on the average boarding times, will help management to adopt a better boarding strategy that in turn will lead to an increase in the number of trips that an aircraft can make.

Keywords: phase type distribution; passenger load factor; computational probability; transportation

MSC: 60J28; 90B06

1. Introduction

The motivation for this work arose from a recent article in the Wall Street Journal [1], as well as personal experience in traveling to many cities, both within the USA and abroad, over the years. In the article, which has the subtitle "Southwest Airlines is studying ways to squeeze more flights per plane—a big focus is on passenger boarding bottlenecks", there is a quote from the airline's *COO* that reads, "If you can collect up enough of these minutes in each turn, then you can start to squeeze out some more flying". Further, the article mentions that boarding times are key to enabling more trips to be performed by the aircraft. This is probably due to the significant variations present in boarding as compared to other aspects, such as cleaning the aircraft before boarding the passengers and the flying time.

A number of articles and research works on this topic have mentioned the bottlenecks involved in the boarding process. For example, in [2], the author mentions that American Airlines uses a single aircraft to make about six or seven trips in a single day. Further, the author lists the activities that occur during the turnaround time, which is the time between the aircraft pulling into the gate with the passengers onboard and the aircraft taking off with a new set of passengers. According to [3], the most significant delays could occur in the boarding process, and the article points out that the boarding time has increased by more than 30% since the 1970s. Moreover, the distribution of the boarding time tends to have a longer tail due to events such as late arrivals of passengers, passengers

needing assistance, and a few last-minute occurences. Thus, a clear understanding of the tail probabilities, namely percentiles, will help the system manager to provide the needed resources.

A number of publications (see, e.g., [4–14]) discuss boarding strategies, such as front-to-back, back-to-front, *WILMA* (window seats board first, followed by middles and aisles), outside-in, reverse pyramid, first-come-first-served, random, or other methods in which boarding is performing by calling each passenger group individually, such as Steffen [12], and changes in the Steffen boarding method. Such strategies may provide insights to determine a strategy that will speed up the boarding process. We refer the reader to [11] for the different boarding methods adopted by a few airlines. In recent times, most airlines have adopted a strategy that ensures that their most loyal customers are treated better compared to others. Loyal customers are the ones who travel frequently and thus accumulate significant award miles to achieve premier status—silver, gold, or platinum (the category name depends on the type of airline). As is known, in any strategy that an airline adopts, there is always randomness involved in the actual boarding process.

Thus, airlines can reduce the time involved in carrying passengers from one city to another by considering various boarding strategies, as well as the boarding times. While there is research (as pointed out earlier) on boarding strategies, to our knowledge, there is no literature on the use of stochastic models to study the effect of a reduction in the average boarding time on the overall performance of the boarding process. The study of such stochastic models is very timely in view of the recent article by the Southwest *COO* in the Wall Street Journal [1]. By building such stochastic models, in this paper, we try to answer questions such as "how much will a reduction in the boarding time result in an increase in the average number of trips made by an aircraft?". With such quantitative descriptions of the reduction in the boarding times' percentiles, management can adopt an appropriate boarding strategy to arrive at a reduction in the average boarding time.

Hence, our aim in this paper is to model the de-boarding–cleaning–boarding–flying sequence, from point A to point B to point A (for circular travel, as seen in many airlines in both local and international flights), using phase type (*PH*) distributions and show the impact of eliminating one minute or more from the average boarding time on key measures involving percentiles. It also seeks to quantify the guaranteed boarding time with a certain level of confidence. We also point out how such modeling can be generalized to include a travel path consisting of more than two cities, which does not always need to be circular. Overall, airline companies are interested in scheduling their flights to maximize the number of trips that an aircraft can make (under ideal conditions), and having a stochastic model to analyze the time will contribute to such planning.

PH-distributions were introduced by Neuts [15] and have been extensively studied in the literature (see, e.g., [16–20]). Recall that a *PH*-distribution is obtained as the time until absorption in an irreducible Markov chain with an absorbing state. In other words, given an irreducible continuous-time Markov chain (*CTMC*) with m transient states and one absorbing state with the generator $\tilde{Q}$ of the form

$$\tilde{Q} = \begin{pmatrix} D & \boldsymbol{d^0} \\ \boldsymbol{0} & 0 \end{pmatrix}, \tag{1}$$

where D of dimension m governs the transitions corresponding to the transient states and the column vector $\boldsymbol{d^0}$ governs the rates of absorption into the absorbing state. Note that this column vector is such that the sum of this and the row sum of D will lead to a zero vector due to the property of the generator of being a *CTMC*. Suppose that the initial probability vector of this *CTMC* is taken as $\boldsymbol{\alpha}$ of dimension m. If X denotes the time until absorption in the *CTMC* starting in one of the m transient states, then the probability distribution of X is said to be a *PH*-distribution with representation given by $(\boldsymbol{\alpha}, D)$ of dimension m. We denote this statement by displaying $X \sim PH(\boldsymbol{\alpha}, D)$ of dimension m.

Its use in stochastic modeling has been amply demonstrated in numerous publications since the seminal paper by Neuts. Very briefly, *PH*-distributions are obtained as the time

until absorption in a finite Markov chain with one absorbing state. These distributions are defined in both discrete and continuous time, and, here, our focus is on the continuous-time version. To completely describe a *PH*-distribution, one needs an initial probability vector and a finite-dimensional matrix that governs the transitions among the transient states. For more details, including properties, examples, and computational aspects, we refer the reader to the above-mentioned references. In particular, we refer to the recent book by Chakravarthy [18] for detailed descriptions with a number of illustrative examples.

This paper is organized as follows. In Section 2, the basic model under study is described, along with its analysis. The analysis of the model in both steady state and a transient one is presented in Section 3. Illustrative numerical examples of the basic model are discussed in Section 4 and concluding remarks are presented in Section 5.

2. Model Description

In this paper, we study boarding times by looking at only two cities, e.g., C_1 and C_2, such that the same aircraft with a capacity to carry N passengers will shuttle back and forth between these two cities. If one is interested in extending this to include multiple-city trips, such as from city C_1 to city C_2 and to city C_3, or to reflect circular paths such as C_1 to city C_2 to city C_3 to city C_1, the model studied here can easily be generalized but with more states to describe the system, and the details are left to the reader.

Generally speaking, the process involved in flying a commercial aircraft is as follows. After landing in a city, the aircraft pulls into the gate and the passengers de-board. The cleaning of the aircraft occurs before a new set of passengers boards the plane. Once the gate closes, the flight is ready to take off, and, after landing in a new city, the process continues. It should be pointed out that while the de-boarding, cleaning, and boarding times depend on the number of passengers, the time from the gate closing to landing in another city does not depend on the number of passengers.

We assume that the vector of the probability mass function (*PMF*) of the number of passengers boarding in city C_1 is given by $\boldsymbol{p_1} = (p_{1,1}, \cdots, p_{1,N})$ and that of the one in city C_2 is $\boldsymbol{p_2} = (p_{2,1}, \cdots, p_{2,N})$. Thus, with probability $p_{1,j}$, the aircraft with a capacity N will leave city C_1 with j passengers onboard. Similarly, with probability $p_{2,j}$, the same aircraft will leave city C_2 with j passengers onboard. In this paper, we place no restriction on the nature of these two *PMF*s. They can be generally distributed (e.g., binomial, truncated geometric, and truncated Poisson) with support on the set $\{1, 2, \cdots, N\}$.

We use *PH*-distributions to model the eight sets of random variables. Generally, the de-boarding, cleaning, and boarding times depend on the number of passengers on the plane; hence, we will model these dependencies by enabling the underlying *PH*-distribution to include another set of parameters. Our analysis here can be modified to model the dependencies under a more general setup using different *PH*-distributions. However, this will increase the number of input distributions significantly. To this end, we define the following (column) vectors of rates.

$$\boldsymbol{\theta_r} = \begin{pmatrix} \theta_{r,1} \\ \vdots \\ \theta_{r,N} \end{pmatrix}, \ 1 \leq r \leq 6. \tag{2}$$

Once again, we place no restriction on the nature of the rate vector, $\boldsymbol{\theta_r}$, $1 \leq r \leq 6$, for our modeling purposes. The following sets of random variables are needed to study the model.

- Define the random variables, $X_1(j)$, $1 \leq j \leq N$, for de-boarding in city C_1 and assume that $X_1(j) \sim PH(\boldsymbol{\beta_1}, \theta_{1,j} S_1)$ of dimension m_1.
- Define the random variables, $X_2(j)$, $1 \leq j \leq N$, for the cleaning of the aircraft while in city C_1 and assume that $X_2(j) \sim PH(\boldsymbol{\beta_2}, \theta_{2,j} S_2)$ of dimension m_2.
- Define the random variables, $X_3(j)$, $1 \leq j \leq N$, for boarding in city C_1 and assume that $X_3(j) \sim PH(\boldsymbol{\beta_3}, \theta_{3,j} S_3)$ of dimension m_3.

- Define the random variable, X_4, to represent the time required for the aircraft to leave the gate in city C_1 and arrive at the gate for de-boarding in city C_2. Let $X_4 \sim PH(\boldsymbol{\beta_4}, S_4)$ of dimension m_4.
- Define the random variables, $X_5(j)$, $1 \leq j \leq N$, for de-boarding in city C_2 and assume that $X_5(j) \sim PH(\boldsymbol{\beta_5}, \theta_{4,j} S_5)$ of dimension m_5.
- Define the random variables, $X_6(j)$, $1 \leq j \leq N$, for the cleaning of the aircraft while in city C_2 and assume that $X_6(j) \sim PH(\boldsymbol{\beta_6}, \theta_{5,j} S_6)$ of dimension m_6.
- Define the random variables, $X_7(j)$, $1 \leq j \leq N$, for boarding in city C_2 and assume that $X_7(j) \sim PH(\boldsymbol{\beta_7}, \theta_{6,j} S_7)$ of dimension m_7.
- Define the random variable, X_8, to represent the time taken for the aircraft to leave the gate in city C_2 and arrive at the gate for de-boarding in city C_1. Let $X_8 \sim PH(\boldsymbol{\beta_8}, S_8)$ of dimension m_8.

In the following, we need the terms below.

- e is a column vector of 1s with appropriate dimensions, which should be clear from the context. Where clarity is needed, the dimensions will be displayed.
- I is an identity matrix of appropriate dimensions. Again, when clarity is needed, the dimensions will be displayed.
- Suppose that a is a vector such that $a = (a_1, \cdots, a_n)$. Then, $\Delta(a)$ denotes a diagonal matrix of dimension n whose ith diagonal element is given by a_i. The inverse, when it exists, of this diagonal matrix will be denoted as $\Delta^{-1}(a)$. In other words, $\Delta^{-1}(a) = [\Delta(a)]^{-1}$.
- The symbols $\otimes$ and $\oplus$, respectively, define the Kronecker product and sum of matrices. A few key works on these can be found in [21–23].

We define a column vector $\boldsymbol{S_i^0}$ of dimension m_i to be such that

$$S_i e + S_i^0 = 0, \ 1 \leq i \leq 8. \tag{3}$$

For use in this work, we define the mean (μ_i'), the variance (σ_i^2), and the invariant vector (δ_i) of the *PH*-renewal process, namely $S_i + S_i^0 \boldsymbol{\beta_i}$, associated with the *PH*-distribution $PH(\boldsymbol{\beta_i}, S_i)$. These quantities are as given below (see, e.g., [18,20]).

$$\mu_i' = \boldsymbol{\beta_i}(-S_i)^{-1} e, \ \sigma_i^2 = 2\boldsymbol{\beta_i}(-S_i)^{-2} e - (\mu_i')^2, \ \delta_i = \frac{1}{\mu_i'} \boldsymbol{\beta_i}(-S_i)^{-1}, \ 1 \leq i \leq 8. \tag{4}$$

3. Analysis of the Model

In this section, we perform the analysis of the model both in time dependence and steady state. The transient analysis will be focused on the boarding event. The reason that we perform the steady-state analysis is that there are some airlines that operate regular flights from city to city (due to constant demands in these sectors) and hence they would be interested in determining how may trips can be made in the long run. With regard to boarding, the transient analysis (i.e., time-dependent study) will shed light on the performance of the boarding process by looking at key measures such as mean, median, and some selected percentiles. Although we focus mainly on the boarding time and the total time for the transient analysis, it is easy to consider other events involved in this process.

In order to study the model using the continuous-time Markov chain (*CTMC*), we need to keep track of the state of the system under study. Before we display the state space of the *CTMC*, we first define a few terms. By $\mathbf{1, 2, 3, 4, 5, 6, 7}$, and $\mathbf{8}$, we define the set of states as

$$\mathbf{1} = \{(\hat{j}_{C_1}, k) : 1 \leq j \leq N, \ 1 \leq k \leq m_1\}, \mathbf{2} = \{(\bar{j}_{C_1}, k) : 1 \leq j \leq N, \ 1 \leq k \leq m_2\},$$
$$\mathbf{3} = \{(\check{j}_{C_1}, k) : 1 \leq j \leq N, \ 1 \leq k \leq m_3\}, \mathbf{4} = \{(j_{C_1}, k) : 1 \leq j \leq N, \ 1 \leq k \leq m_4\}$$
$$\mathbf{5} = \{(\hat{j}_{C_2}, k) : 1 \leq j \leq N, \ 1 \leq k \leq m_5\}, \mathbf{6} = \{(\bar{j}_{C_2}, k) : 1 \leq j \leq N, \ 1 \leq k \leq m_6\},$$
$$\mathbf{7} = \{(\check{j}_{C_2}, k) : 1 \leq j \leq N, \ 1 \leq k \leq m_7\}, \mathbf{8} = \{(\tilde{j}_{C_2}, k) : 1 \leq j \leq N, \ 1 \leq k \leq m_8\},$$

where, for $1 \leq j \leq N$,

- $(\hat{j}_{C_1}, k)$ corresponds to the de-boarding process in city C_1 (after the aircraft has landed with j passengers onboard) and the phase is k;
- $(\bar{j}_{C_1}, k)$ corresponds to the aircraft (which originally had j passengers onboard) being cleaned while in city C_1 and the phase is in k;
- $(\tilde{j}_{C_1}, k)$ corresponds to the boarding process in city C_1 when the aircraft is to leave with j passengers onboard and the phase is in k;
- (j_{C_1}, k) corresponds to the state in which the aircraft is on its way to city C_2 and the phase is in k; note that we need to keep track of the number of passengers onboard even though the traveling time is not dependent on the number onboard since the de-boarding time in city C_2 depends on this number;
- The other states, $(\hat{j}_{C_2}, k)$, $(\bar{j}_{C_2}, k)$, $(\tilde{j}_{C_2}, k)$, and (j_{C_2}, k), are similarly defined by replacing city C_1 with C_2 and vice versa in the above definitions.

Noting that the system, at any given time, can only be in one of eight sets of states (corresponding to the state of the aircraft, such as de-boarding/boarding/cleaning/leaving city C_1 or de-boarding/boarding/cleaning/leaving city C_2), the state space, Ω, is given by

$$\Omega = \{\mathbf{1}, \mathbf{2}, \mathbf{3}, \mathbf{4}, \mathbf{5}, \mathbf{6}, \mathbf{7}, \mathbf{8}\}. \tag{5}$$

The generator, Q, of the *CTMC* is given by

$$Q = \begin{array}{c} \\ \mathbf{1} \\ \mathbf{2} \\ \mathbf{3} \\ \mathbf{4} \\ \mathbf{5} \\ \mathbf{6} \\ \mathbf{7} \\ \mathbf{8} \end{array} \begin{array}{c} \begin{matrix} \mathbf{1} & \mathbf{2} & \mathbf{3} & \mathbf{4} & \mathbf{5} & \mathbf{6} & \mathbf{7} & \mathbf{8} \end{matrix} \\ \left(\begin{matrix} A_1 & A_{1,1} & & & & & & \\ & A_2 & A_{2,1} & & & & & \\ & & A_3 & A_{3,1} & & & & \\ & & & A_4 & A_{4,1} & & & \\ & & & & A_5 & A_{5,1} & & \\ & & & & & A_6 & A_{6,1} & \\ & & & & & & A_7 & A_{7,1} \\ A_{8,1} & & & & & & & A_8 \end{matrix} \right) \end{array}, \tag{6}$$

where the entries of Q are as given below:

$$A_1 = \Delta(\boldsymbol{\theta_1}) \otimes S_1, \ A_{1,1} = \Delta(\boldsymbol{\theta_1}) \otimes S_1^0 \boldsymbol{\beta_2}, \ A_2 = \Delta(\boldsymbol{\theta_2}) \otimes S_2, \ A_{2,1} = \boldsymbol{\theta_2}\, p_1 \otimes S_2^0 \boldsymbol{\beta_3},$$

$$A_3 = \Delta(\boldsymbol{\theta_3}) \otimes S_3, \ A_{3,1} = \Delta(\boldsymbol{\theta_3}) \otimes S_3^0 \boldsymbol{\beta_4}, \ A_4 = I \otimes S_4, \ A_{4,1} = I \otimes S_4^0 \boldsymbol{\beta_5},$$

$$A_5 = \Delta(\boldsymbol{\theta_4}) \otimes S_5, \ A_{5,1} = \Delta(\boldsymbol{\theta_4}) \otimes S_5^0 \boldsymbol{\beta_6}, \ A_6 = \Delta(\boldsymbol{\theta_5}) \otimes S_6, \ A_{6,1} = \boldsymbol{\theta_5}\, p_2 \otimes S_6^0 \boldsymbol{\beta_7}, \tag{7}$$

$$A_7 = \Delta(\boldsymbol{\theta_6}) \otimes S_7, \ A_{7,1} = \Delta(\boldsymbol{\theta_6}) \otimes S_7^0 \boldsymbol{\beta_8}, \ A_8 = I \otimes S_8, \ A_{8,1} = I \otimes S_8^0 \boldsymbol{\beta_1}.$$

3.1. Steady-State Analysis

Let $\boldsymbol{u} = (\boldsymbol{u_1}, \cdots, \boldsymbol{u_8})$ denote the steady-state probability vector of Q. In particular, $\boldsymbol{u}$ satisfies

$$\boldsymbol{u}Q = \mathbf{0}, \ \ \boldsymbol{u}e = 1. \tag{8}$$

For later use, we further partition $\boldsymbol{u_i}$, for $1 \leq i \leq 8$, as $\boldsymbol{u_i} = (\boldsymbol{u_{i,1}}, \cdots, \boldsymbol{u_{i,N}})$. Note that the vector $\boldsymbol{u_{i,j}}$ of dimension m_i, for $1 \leq j \leq N$, gives the steady-state probability vector of the underling process to be in state (i, j). The following theorem gives an explicit expression for the vector $\boldsymbol{u}$.

Theorem 1. *The vector $\boldsymbol{u}$ is explicitly given by*

$$\boldsymbol{u_1} = d\mu_1'(\boldsymbol{p_2}\Delta^{-1}(\boldsymbol{\theta_1}) \otimes \boldsymbol{\delta_1}), \boldsymbol{u_2} = d\mu_2'(\boldsymbol{p_2}\Delta^{-1}(\boldsymbol{\theta_2}) \otimes \boldsymbol{\delta_2}), \boldsymbol{u_3} = d\mu_3'(\boldsymbol{p_1}\Delta^{-1}(\boldsymbol{\theta_3}) \otimes \boldsymbol{\delta_3}),$$

$$\boldsymbol{u_4} = d\mu_4'(\boldsymbol{p_1} \otimes \boldsymbol{\delta_4}), \boldsymbol{u_5} = d\mu_5'(\boldsymbol{p_1}\Delta^{-1}(\boldsymbol{\theta_4}) \otimes \boldsymbol{\delta_5}), \boldsymbol{u_6} = d\mu_6'(\boldsymbol{p_1}\Delta^{-1}(\boldsymbol{\theta_5}) \otimes \boldsymbol{\delta_6}), \quad (9)$$

$$\boldsymbol{u_7} = d\mu_7'(\boldsymbol{p_2}\Delta^{-1}(\boldsymbol{\theta_6}) \otimes \boldsymbol{\delta_7}), \boldsymbol{u_8} = d\mu_8'(\boldsymbol{p_2} \otimes \boldsymbol{\delta_8}),$$

where the invariant vectors $\boldsymbol{\delta_i}$, $1 \leq i \leq 8$, are as given in Equation (4) and the constant d is given by

$$d = \left[\mu_1'\boldsymbol{p_2}\Delta^{-1}(\boldsymbol{\theta_1})\boldsymbol{e} + \mu_2'\boldsymbol{p_2}\Delta^{-1}(\boldsymbol{\theta_2})\boldsymbol{e} + \mu_3'\boldsymbol{p_1}\Delta^{-1}(\boldsymbol{\theta_3})\boldsymbol{e} + \mu_4' \right.$$
$$\left. +\mu_5'\boldsymbol{p_1}\Delta^{-1}(\boldsymbol{\theta_4})\boldsymbol{e} + \mu_6'\boldsymbol{p_1}\Delta^{-1}(\boldsymbol{\theta_5})\boldsymbol{e} + \mu_7'\boldsymbol{p_2}\Delta^{-1}(\boldsymbol{\theta_6})\boldsymbol{e} + \mu_8' \right]^{-1}. \quad (10)$$

Proof. Using the properties of the Kronecker product (see, e.g., [18,21,23]) and the invariant vectors given in Equation (4), the steady-state equations given in Equation (8) can be written as

$$\boldsymbol{u_1} = \mu_1'\boldsymbol{u_8}(\Delta^{-1}(\boldsymbol{\theta_1}) \otimes S_8^0 \boldsymbol{\delta_1}), \quad \boldsymbol{u_2} = \mu_2'\boldsymbol{u_1}(\Delta(\boldsymbol{\theta_1})\Delta^{-1}(\boldsymbol{\theta_2}) \otimes S_1^0 \boldsymbol{\delta_2}),$$

$$\boldsymbol{u_3} = \mu_3'\boldsymbol{u_2}(\boldsymbol{\theta_2}\,\boldsymbol{p_1}\Delta^{-1}(\boldsymbol{\theta_3}) \otimes S_2^0 \boldsymbol{\delta_3}), \quad \boldsymbol{u_4} = \mu_4'\boldsymbol{u_1}(\Delta(\boldsymbol{\theta_3}) \otimes S_3^0 \boldsymbol{\delta_4}),$$

$$\boldsymbol{u_5} = \mu_5'\boldsymbol{u_4}(\Delta^{-1}(\boldsymbol{\theta_4}) \otimes S_4^0 \boldsymbol{\delta_5}), \quad \boldsymbol{u_6} = \mu_6'\boldsymbol{u_5}(\Delta(\boldsymbol{\theta_4})\Delta^{-1}(\boldsymbol{\theta_5}) \otimes S_5^0 \boldsymbol{\delta_6}), \quad (11)$$

$$\boldsymbol{u_7} = \mu_7'\boldsymbol{u_6}(\boldsymbol{\theta_5}\,\boldsymbol{p_2}\Delta^{-1}(\boldsymbol{\theta_6}) \otimes S_6^0 \boldsymbol{\delta_7}), \quad \boldsymbol{u_8} = \mu_8'\boldsymbol{u_7}(\Delta(\boldsymbol{\theta_6}) \otimes S_7^0 \boldsymbol{\delta_8}), \quad \sum_{i=1}^{8} \boldsymbol{u_i}\boldsymbol{e} = 1.$$

From the equations given in (11), it is easy to verify, for $1 \leq j \leq N$, that

$$u_{1,j} = \frac{\mu_1'}{\theta_{1,j}}u_{8,j}S_8^0 \boldsymbol{\delta_1}, \quad u_{2,j} = \frac{\mu_2'\theta_{1,j}}{\theta_{2,j}}u_{1,j}S_1^0 \boldsymbol{\delta_2}, \quad u_{3,j} = \frac{\mu_3'p_{1,j}}{\theta_{3,j}}\sum_{k=1}^{N}\theta_{2,k}u_{2,k}S_2^0 \boldsymbol{\delta_3},$$

$$u_{4,j} = \mu_4'\theta_{3,j}u_{3,j}S_3^0 \boldsymbol{\delta_4}, \quad u_{5,j} = \frac{\mu_5'}{\theta_{4,j}}, \quad u_{4,j}S_4^0 \boldsymbol{\delta_5}, \quad u_{6,j} = \frac{\mu_6'\theta_{4,j}}{\theta_{5,j}}u_{5,j}S_5^0 \boldsymbol{\delta_6}, \quad (12)$$

$$u_{7,j} = \frac{\mu_7'p_{2,j}}{\theta_{6,j}}\sum_{k=1}^{N}\theta_{5,k}u_{6,k}S_6^0 \boldsymbol{\delta_7}, \quad u_{8,j} = \mu_8'\theta_{6,j}u_{7,j}S_7^0 \boldsymbol{\delta_8},$$

from which we obtain

$$\theta_{1,j}u_{1,j}S_1^0 = \theta_{2,j}u_{2,j}S_2^0 = u_{8,j}S_8^0,$$

$$\theta_{3,j}u_{3,j}S_3^0 = u_{4,j}S_4^0 = \theta_{4,j}u_{5,j}S_5^0 = \theta_{5,j}u_{6,j}S_6^0 = p_{1,j}\sum_{k=1}^{N}u_{8,k}S_8^0,$$

$$(13)$$

$$\theta_{6,j}u_{7,j}S_7^0 = u_{8,j}S_8^0 = p_{2,j}\sum_{k=1}^{N}u_{8,k}S_8^0.$$

The stated result follows from Equations (12) and (13) and the normalizing condition given in (11). □

Suppose that W_1, W_2, W_3, and W_4, respectively, denote the times spent in de-boarding the plane, cleaning the plane, boarding the plane, and leaving city C_1 given that the aircraft starts in this particular mode. In other words, W_1 is the random variable keeping track of the time that it takes to de-board the plane in city C_1 given that de-boarding has started. Similarly, let W_5, W_6, W_7, and W_8, respectively, denote the time spent in de-boarding the

plane, cleaning the plane, boarding the plane, and leaving in city C_2. Then, the following result shows that these random variables are all of the *PH* type.

Theorem 2. *The random variables, W_i, $1 \le i \le 8$, follow PH-distributions with representations given as*

$$W_1 \sim (p_2 \otimes \beta_1, A_1), \ W_2 \sim (p_2 \otimes \beta_2, A_2), \ W_3 \sim (p_1 \otimes \beta_3, A_3), \ W_4 \sim (\beta_4, S_4), \\ W_5 \sim (p_1 \otimes \beta_5, A_5), \ W_6 \sim (p_1 \otimes \beta_6, A_6), \ W_7 \sim (p_2 \otimes \beta_7, A_7), \ W_4 \sim (\beta_8, S_8). \quad (14)$$

Proof. Let γ denote the conditional probability that de-boarding starts in city C_1. This conditional probability is obtained by looking at the sequence starting with the cleaning of the aircraft at city C_2, which is then followed by the boarding of the aircraft and then the plane leaving the city at an arbitrary time. It is easy to verify that

$$\gamma = d_1 u_6 (-A_6)^{-1} A_{6,1} (-A_7)^{-1} A_{7,1} (-A_8)^{-1} A_{8,1} = d_1 d \mu_6' (p_1 \Delta^{-1}(\theta_5) e)(p_2 \otimes \beta_1), \quad (15)$$

where d_1 is the normalizing constant. Thus, the time spent in the de-boarding state in city C_1 is of the *PH* type with the representation given in Equation (14). In a similar manner, we obtain the other representations. It is worth pointing out that the reason for the smaller-dimension representation for W_4 and W_8 is due to the fact that the flying time does not depend on the number of passengers onboard the aircraft, unlike the other times. $\square$

Corollary 1. *The mean (μ_{W_i}') and the standard deviation (σ_{W_i}') of W_i, $1 \le i \le 8$, are obtained explicitly as follows. In the following, we use the notation ξ_i for the second moment of X_i, $1 \le i \le 8$. In other words, $\xi_i = 2\beta_i e(-S_i)^{-2} e$, $1 \le i \le 8$.*

$$\mu_{W_1}' = \mu_1' p_2 \Delta^{-1}(\theta_1) e, \ \sigma_{W_1}' = \xi_1 p_2 \Delta^{-2}(\theta_1) e - (\mu_{W_1}')^2,$$

$$\mu_{W_2}' = \mu_2' p_2 \Delta^{-1}(\theta_2) e, \ \sigma_{W_2}' = \xi_2 p_2 \Delta^{-2}(\theta_2) e - (\mu_{W_2}')^2,$$

$$\mu_{W_3}' = \mu_3' p_1 \Delta^{-1}(\theta_3) e, \ \sigma_{W_3}' = \xi_3 p_1 \Delta^{-3}(\theta_3) e - (\mu_{W_3}')^2, \ \mu_{W_4}' = \mu_4', \ \sigma_{W_4}' = (\sigma_{W_4}')^2,$$

$$\mu_{W_5}' = \mu_5' p_1 \Delta^{-1}(\theta_4) e, \ \sigma_{W_5}' = \xi_5 p_1 \Delta^{-2}(\theta_4) e - (\mu_{W_5}')^2, \quad (16)$$

$$\mu_{W_6}' = \mu_6' p_1 \Delta^{-1}(\theta_5) e, \ \sigma_{W_6}' = \xi_6 p_1 \Delta^{-2}(\theta_5) e - (\mu_{W_6}')^2,$$

$$\mu_{W_7}' = \mu_7' p_2 \Delta^{-1}(\theta_6) e, \ \sigma_{W_7}' = \xi_7 p_2 \Delta^{-2}(\theta_6) e - (\mu_{W_7}')^2, \ \mu_{W_8}' = \mu_8', \ \sigma_{W_8}' = (\sigma_{W_8}')^2.$$

Note 1. *It is worth pointing out that the means of W_i are related to the probabilities u_i, for $1 \le i \le 8$, as $\mu_{W_i}' = d u_i e$, where d is as given in Equation (10).*

Suppose that T is the total time starting from city C_1 until returning to city C_1. Then, we have the following result.

Theorem 3. *The random variable, T, follows a PH-distribution with representation $((p_2 \otimes \beta_1, \mathbf{0}), A)$ of order $m_8 + N \sum_{i=1}^{7} m_i$, where A is given by*

$$A = \begin{bmatrix} A_1 & A_{1,1} & & & & & & \\ & A_2 & A_{2,1} & & & & & \\ & & A_3 & A_{3,1} & & & & \\ & & & A_4 & A_{4,1} & & & \\ & & & & A_5 & A_{5,1} & & \\ & & & & & A_6 & A_{6,1} & \\ & & & & & & A_7 & (\theta_6 \otimes S_7^0 \beta_8) \\ & & & & & & & S_8 \end{bmatrix}, \quad (17)$$

and the matrices appearing in A are as given in Equation (7). Further, the mean and the variance of T are given by

$$\mu'_T = \frac{1}{d},$$

$$
\begin{aligned}
\sigma^2_T = {}& \mu'_1 \xi_1 p_2 \Delta^{-2}(\theta_1)e + \mu'_2 \left[\xi_2 p_2 \Delta^{-2}(\theta_2)e + \mu'_1 \Delta^{-1}(\theta_1)\Delta^{-1}(\theta_2)e \right] \\
&+ \mu'_3 \left[\xi_3 p_1 \Delta^{-2}(\theta_3)e + p_1 \Delta^{-1}(\theta_3)e(\mu'_{W_1} + \mu'_{W_2}) \right] + \mu'_4 \left[\xi_4 + \sum_{r=1}^{3} \mu'_{W_r} \right] \\
&+ \mu'_5 \left[\xi_5 p_1 \Delta^{-2}(\theta_4)e + \mu'_4 p_1 \Delta^{-1}(\theta_4)e + \mu'_3 \Delta^{-1}(\theta_3)\Delta^{-1}(\theta_4)e \right] \\
&+ \mu'_5 (\mu'_{W_1} + \mu'_{W_2}) p_1 \Delta^{-1}(\theta_4)e + \mu'_6 \left[\xi_6 p_1 \Delta^{-2}(\theta_5)e + \mu'_5 p_1 \Delta^{-1}(\theta_4)\Delta^{-1}(\theta_5)e \right] \\
&+ \mu'_6 \left[\mu'_4 p_1 \Delta^{-1}(\theta_5)e + \mu'_3 p_1 \Delta^{-1}(\theta_3)\Delta^{-1}(\theta_5)e + p_1 \Delta^{-1}(\theta_5)e(\mu'_{W_1} + \mu'_{W_2}) \right] \\
&+ \mu'_7 \left[\xi_7 p_2 \Delta^{-2}(\theta_6)e + p_2 \Delta^{-1}(\theta_6)e \sum_{i=1}^{6} \mu'_{W_i} \right] + \mu'_8 \left[\xi_8 + \sum_{i=1}^{7} \mu'_{W_i} \right] - \left(\frac{1}{d} \right)^2.
\end{aligned}
\tag{18}
$$

Proof. First, we define two vectors, a and b, as

$$a = (p_2 \otimes \beta_1, 0)(-A)^{-1}, \quad b = a(-A)^{-1}, \tag{19}$$

so that

$$\mu'_T = a(-A)^{-1}e, \quad \sigma^2_T = 2b(-A)^{-1}e - (\mu'_T)^2. \tag{20}$$

It should be pointed out that while we can obtain μ'_T as $\mu'_T = \sum_{i=1}^{8} \mu'_{W_i}$, one needs to exploit the structure of A to obtain σ^2_T. The latter is due to the fact that the variance of T cannot be obtained as the sum of the variances of W_i, $1 \leq i \leq 8$, due to the possible dependencies of these random variables within themselves. In order to obtain this variance, we need to obtain the vector b, which depends on a. Moreover, one can use the vector a as part of an internal accuracy check. Partitioning

$$a = (a_1, \cdots, a_N), \quad b = (b_1, \cdots, b_N), \tag{21}$$

and rewriting the equation $a = (p_2 \otimes \beta_1, 0)(-A)^{-1}$ as

$$a(-A) = (p_2 \otimes \beta_1, 0), \tag{22}$$

it is easy to verify, by exploiting the sparsity of the coefficient matrices, the following expressions for the vector a.

$$a_1 = \mu'_1 (p_2 \Delta^{-1}(\theta_1) \otimes \delta_1), \quad a_2 = \mu'_2 (p_2 \Delta^{-1}(\theta_2) \otimes \delta_2), \quad a_3 = \mu'_3 (p_1 \Delta^{-1}(\theta_3) \otimes \delta_3),$$

$$a_4 = \mu'_4 (p_1 \otimes \delta_4), \quad a_5 = \mu'_5 (p_1 \Delta^{-1}(\theta_4) \otimes \delta_5), \quad a_6 = \mu'_6 (p_1 \Delta^{-1}(\theta_5) \otimes \delta_6), \tag{23}$$

$$a_7 = \mu'_7 (p_2 \Delta^{-1}(\theta_6) \otimes \delta_7), \quad a_8 = \mu'_8 \delta_8,$$

where the invariant vectors δ_i, $1 \leq i \leq 8$, are as given in Equation (4). Thus, we see

$$\mu'_T = \sum_{i=1}^{8} a_i e, \tag{24}$$

and, upon using Equations (23) and (10), we obtain the stated result for μ'_T.

Having obtained the expressions for a, we once again exploit the structure of the matrix A to obtain the expressions for b. It is easy to verify that, for $1 \le j \le N$, we have

$$
\begin{aligned}
& b_{1,j} = \frac{1}{\theta_{1,j}} a_{1,j}(-S_1)^{-1}, \ b_{2,j} = \frac{1}{\theta_{2,j}} \Big[a_{2,j} + a_{1,j} e\, \beta_2 \Big] (-S_2)^{-1}, \\
& b_{3,j} = \frac{1}{\theta_{3,j}} \Big[a_{3,j} + p_{1,j}(a_1 e + a_2 e)\beta_3 \Big] (-S_3)^{-1}, \\
& b_{4,j} = \Big[a_{4,j} + (a_{3,j} e + p_{1,j}[a_1 e + a_2 e])\beta_4 \Big] (-S_4)^{-1}, \\
& b_{5,j} = \frac{1}{\theta_{4,j}} \Big[a_{5,j} + (a_{4,j} e + a_{3,j} e + p_{1,j}[a_1 e + a_2 e])\beta_5 \Big] (-S_5)^{-1}, \\
& b_{6,j} = \frac{1}{\theta_{5,j}} \Big[a_{6,j} + (a_{5,j} e + a_{4,j} e + a_{3,j} e + p_{1,j}[a_1 e + a_2 e])\beta_6 \Big] (-S_6)^{-1}, \\
& b_{7,j} = \frac{1}{\theta_{6,j}} \Big[a_{7,j} + p_{2,j} \Big(\sum_{i=1}^{6} a_i e \Big) \beta_7 \Big] (-S_7)^{-1}, \ b_8 = \Big[a_8 + \Big(\sum_{i=1}^{7} a_i e \Big) \beta_8 \Big] (-S_8)^{-1},
\end{aligned}
\tag{25}
$$

from which the stated result follows immediately. □

Note 2. *Suppose that one is interested in looking at the time, V, that it takes to travel from city C_1 (from the instant that de-boarding starts) to city C_2 (reaching the gate). Similarly to Theorem 3, it is easy to see that V follows a PH-distribution with representation $((p_2 \otimes \beta_1, 0), B)$ of order $m_4 + N \sum_{i=1}^{3} m_i$, where B is given by*

$$
B = \begin{bmatrix}
A_1 & A_{1,1} & & \\
& A_2 & A_{2,1} & \\
& & A_3 & (\theta_3 \otimes S_3^0)\beta_4 \\
& & & S_4
\end{bmatrix},
\tag{26}
$$

and the entries of B are as given in Equation (7). The mean and the standard deviation of V can be obtained similarly and the details are omitted.

3.2. Transient Analysis

In this section, we perform a transient analysis with the main focus on the boarding time. However, we will briefly outline the analysis of the other events for the sake of completeness.

From Theorem 2, it is easy to verify (see, e.g., [18–20]) that the *PDF*, e.g., $f_i(t)$, and the cumulative probability distribution function (*CDF*), e.g., $F_i(t)$, for the random variable W_i, for $1 \le i \le 8$, are given as

$$
\begin{aligned}
& f_1(t) = \sum_{j=1}^{N} p_{2,j}\theta_{1,j}\beta_1 e^{\theta_{1,j}S_1 t} S_1^0, \ F_1(t) = 1 - \sum_{j=1}^{N} p_{2,j}\beta_1 e^{\theta_{1,j}S_1 t} e, \ t \ge 0, \\
& f_2(t) = \sum_{j=1}^{N} p_{2,j}\theta_{2,j}\beta_2 e^{\theta_{2,j}S_2 t} S_2^0, \ F_2(t) = 1 - \sum_{j=1}^{N} p_{2,j}\beta_2 e^{\theta_{2,j}S_2 t} e, \ t \ge 0, \\
& f_3(t) = \sum_{j=1}^{N} p_{1,j}\theta_{3,j}\beta_3 e^{\theta_{3,j}S_3 t} S_3^0, \ F_3(t) = 1 - \sum_{j=1}^{N} p_{1,j}\beta_3 e^{\theta_{3,j}S_3 t} e, \ t \ge 0, \\
& \qquad\qquad f_4(t) = \beta_4 e^{S_4 t} S_4^0, \ F_4(t) = 1 - \beta_4 e^{S_4 t} e, \ t \ge 0, \\
& f_5(t) = \sum_{j=1}^{N} p_{1,j}\theta_{4,j}\beta_5 e^{\theta_{4,j}S_5 t} S_5^0, \ F_5(t) = 1 - \sum_{j=1}^{N} p_{1,j}\beta_5 e^{\theta_{5,j}S_1 t} e, \ t \ge 0, \\
& f_6(t) = \sum_{j=1}^{N} p_{1,j}\theta_{5,j}\beta_6 e^{\theta_{5,j}S_6 t} S_6^0, \ F_6(t) = 1 - \sum_{j=1}^{N} p_{1,j}\beta_6 e^{\theta_{5,j}S_6 t} e, \ t \ge 0, \\
& f_7(t) = \sum_{j=1}^{N} p_{2,j}\theta_{6,j}\beta_7 e^{\theta_{2,j}S_7 t} S_7^0, \ F_7(t) = 1 - \sum_{j=1}^{N} p_{1,j}\beta_7 e^{\theta_{6,j}S_7 t} e, \ t \ge 0, \\
& \qquad\qquad f_8(t) = \beta_8 e^{S_8 t} S_8^0, \ F_8(t) = 1 - \beta_8 e^{S_8 t} e, \ t \ge 0.
\end{aligned}
\tag{27}
$$

The above functions can be computed easily using the algorithmic procedures published in the literature (see, e.g., [18,19]). Moreover, for any special cases of *PH*-distributions, such as Erlang or hyperexponential, the calculations can further be simplified.

While implementing the algorithm to compute the *CDF*, we can also compute various quartiles to supplement the mean and the standard deviation of the random variables, W_i, $1 \leq i \leq 8$. Specifically, we discuss these measures for the boarding times in Section 4.

Using Theorem 3, we can compute the *PDF* and *CDF* of T and V as

$$f_T(t) = (\boldsymbol{p_2} \otimes \boldsymbol{\beta_1}, \boldsymbol{0})e^{At}\boldsymbol{A^0}, \quad F_T(t) = 1 - (\boldsymbol{p_2} \otimes \boldsymbol{\beta_1}, \boldsymbol{0})e^{At}\boldsymbol{e}, \quad t \geq 0, \tag{28}$$

and

$$f_V(t) = (\boldsymbol{p_2} \otimes \boldsymbol{\beta_1}, \boldsymbol{0})e^{Vt}\boldsymbol{V^0}, \quad F_V(t) = 1 - (\boldsymbol{p_2} \otimes \boldsymbol{\beta_1}, \boldsymbol{0})e^{Vt}\boldsymbol{e}, \quad t \geq 0, \tag{29}$$

where $\boldsymbol{A^0}$ and $\boldsymbol{V^0}$ are such that $A\boldsymbol{e} + \boldsymbol{A^0} = \boldsymbol{0}$ and $V\boldsymbol{e} + \boldsymbol{V^0} = \boldsymbol{0}$.

Note that when using a general *PH*-distribution to compute the exponential matrix needed in the *PDF* and *CDF*, one can use the uniformization method (see, e.g., [18]). Here, we will briefly list the steps involved in the computation of the *PDF* and *CDF* of V (Algorithm 1).

Algorithm 1: Algorithmic Steps to Compute $f_V(t)$ and $F_V(t)$ Using Uniformization Method.

Step 0: Compute $\eta = \max_i |V_{i,i}|$. That is, η is the maximum of the diagonal elements of the matrix V. Note that η is required for the computation of the *PDF* and *CDF* over a specified set of values, e.g., $\{t_1, \cdots, t_n\}$. Let $P = I + \dfrac{1}{\eta}V$. Let ϵ be a small positive number.

Step 1: For a given t, compute $\zeta_r = e^{-\eta t}\dfrac{(\eta t)^r}{r!}$, $0 \leq r \leq r^*$, where $r^* = r^*(t)$ is such that $\sum\limits_{r=0}^{r^*} \zeta_r > 1 - \epsilon$. Let $i = 0$, $\boldsymbol{h^{(0)}} = (\boldsymbol{p_2} \otimes \boldsymbol{\beta_1}, \boldsymbol{0})$, $\varphi^{(0)} = 1 - \zeta_0$, and $g^{(0)} = \zeta_0 \boldsymbol{h^{(0)}}\boldsymbol{V^0}$.

Step 2: $i \leftarrow i + 1$, $\boldsymbol{h^{(i)}} = \boldsymbol{h^{(i-1)}}P$, $\varphi^{(i)} = \varphi^{(i-1)} - \zeta_i \boldsymbol{h^{(i)}}\boldsymbol{e}$, and $g^{(i)} = g^{(i-1)} + \zeta_i \boldsymbol{h^{(i)}}\boldsymbol{V^0}$.

Step 3: If $i < r^*$, go to Step 2.

Step 4: $f_V(t) = g^{(r^*)}$ and $F_V(t) = \varphi^{(r^*)}$.

Note 3. *It is worth pointing out that the unique structure of V and hence P should be exploited in the steps mentioned above. This is very important, especially when N is large, as well as when the orders of the underlying PH-representations are large. The key steps are outlined below.*

Observing that $\boldsymbol{h^{(0)}} = (\boldsymbol{p_2} \otimes \boldsymbol{\beta_1}, \boldsymbol{0})$ and partitioning $\boldsymbol{h^{(i)}}$ as

$$\boldsymbol{h^{(i)}} = (\boldsymbol{h_1^{(i)}}, \cdots, \boldsymbol{h_N^{(i)}}), \quad 1 \leq i \leq 3, \, i \geq 0, \tag{30}$$

we proceed as follows. Given the current iterate value $\boldsymbol{h^{(k)}}$ for $k = i - 1$, the next iterate value for $k = i$ is obtained as

$$\boldsymbol{h_{1,j}^{(i)}} = \boldsymbol{h_{1,j}^{(i-1)}} + \frac{1}{\eta}\theta_{1,j}\boldsymbol{h_{1,j}^{(i-1)}}S_1, \, 1 \leq j \leq N, \tag{31}$$

$$\boldsymbol{h_{2,j}^{(i)}} = \boldsymbol{h_{2,j}^{(i-1)}} + \frac{1}{\eta}\Big[\theta_{1,j}\boldsymbol{h_{1,j}^{(i-1)}}S_1^0\boldsymbol{\beta_2} + \theta_{2,j}\boldsymbol{h_{2,j}^{(i-1)}}S_2\Big], \, 1 \leq j \leq N, \tag{32}$$

$$\boldsymbol{h_{3,j}^{(i)}} = \boldsymbol{h_{3,j}^{(i-1)}} + \frac{1}{\eta}\Big[p_{1,j}\sum_{k=1}^{N}\theta_{2,k}\boldsymbol{h_{2,k}^{(i-1)}}S_2^0\boldsymbol{\beta_3} + \theta_{3,j}\boldsymbol{h_{3,j}^{(i-1)}}S_3\Big], \, 1 \leq j \leq N, \tag{33}$$

$$h_4^{(i)} = h_4^{(i-1)} + \frac{1}{\eta}\left[\sum_{k=1}^{N}\theta_{3,k}h_{3,k}^{(i-1)}S_3^0\beta_4 + h_4^{(i-1)}S_4\right]. \tag{34}$$

One can further exploit any unique structure for the matrices S_i, $1 \leq i \leq 4$. For example, when dealing with a hyperexponential distribution, the corresponding matrix in the PH-representation is a diagonal matrix and this will help to further exploit this structure. The details are omitted.

3.3. Extension to More than Two Cities

The approach taken for two cities can easily be extended to more than two cities. However, the dimensions of the problem increase. For example, if there are K cities involved, then, instead of using 8 random variables to describe the process for the two-city case, we need $4K$ random variables. The results that are true for the two-city case will also hold but with larger-dimension representations for the underlying random variables.

4. Illustrative Numerical Examples

In this section, we illustrate the key concepts with two sets of numerical examples. The time units, unless otherwise specified, are hours. The input parameters for the illustrative examples are chosen as follows. In the airline industry, the *passenger load factor* (*PLF*) [24] is defined as the ratio of the number of actual passengers to the number of available seats. We will denote this fraction as p in the following. Based on the data provided in [24], we note that this fraction (for domestic flights) ranges from 0.55 to 0.85 approximately. Thus, we conduct our analysis by taking *PLF* to be in this range. However, here, we discuss the examples by fixing p at 0.55 and 0.85.

It would be ideal to perform analyses with all practical data for the model studied here. However, except for *PLF*, to our knowledge, there are no data on boarding times available to use here. It is possible that these data are protected by each airline and are not available to the public. When these data are made available or when an airline wishes to explore the use of the model proposed here, one can fit the data to a *PH*-distribution (see, e.g., [25–32]). For the *PMF* of the number of passengers, we consider truncated binomial, truncated (reverse) geometric, and truncated Poisson forms. In particular, we take p_1 and p_2 to be one of the following three discrete distributions.

Truncated binomial (*B*): This is a binomial distribution that is truncated so that the mass is within $\{1, \cdots, N\}$. Specifically, the *PMF* is of the form

$$\frac{1}{\left[1 - (1 - p_b)^N\right]}\binom{N}{n}p_b^n(1 - p_b)^{N-n}, \; n = 1, \cdots, N. \tag{35}$$

Truncated geometric (*G*): This is a (reversed) geometric distribution that is truncated so that the mass is within $\{1, \cdots, N\}$. Specifically, the *PMF* is of the form

$$\frac{1}{\left[1 - (1 - p_g)^N\right]}p_g(1 - p_g)^{N-n}, \; n = 1, \cdots, N. \tag{36}$$

Truncated Poisson (*P*): This is a Poisson distribution that is truncated so that the mass is within $\{1, \cdots, N\}$. Specifically, the *PMF* is of the form

$$c\,e^{-\lambda}\frac{\lambda^n}{n!}, \; n = 1, \cdots, N, \tag{37}$$

where c is the normalizing constant to ensure a legitimate *PMF*.

In order to compare the various scenarios (when varying the type of *PMF*), we have to choose the parameters of the above-mentioned *PMF* in such a way that the mean number of passengers will always be the same. For example, if $N = 100$ and $p = 0.55$, then the mean number of passengers onboard will be 55. Thus, to arrive at this mean for the truncated binomial, one has to choose $p_b = p$, $p_g = 0.0054$, and $\lambda = 55$. It is worth mentioning

that, due to the size of N and the values of p considered for the illustrative examples, the truncated binomial reduces to the binomial one since $(1 - p_b)^N \simeq 0$.

It should be pointed out that when computing the binomial probabilities, one can encounter overflow or underflow issues, especially when N is large. To avoid this, one should find the mode of the binomial distribution and then compute the rest of the probabilities recursively. To facilitate such computation, we provide the mode values for the binomial case. For the set of parameters considered in this section, Table 1 lists the corresponding parameter values.

Table 1. Parameter values for *PMF*.

p	N	Binomial (Mode)	Geometric	Poisson
	50	0.1119	0.0096	27.5010
	100	0.0800	0.0054	55.0000
	150	0.0652	0.0037	82.5000
0.55	200	0.0566	0.0029	110.0000
	250	0.0506	0.0023	137.5000
	300	0.0463	0.0019	165.0000
	350	0.0428	0.0017	192.5000
	400	0.0401	0.0015	220.0000
	50	0.1575	0.1162	44.8805
	100	0.1111	0.0618	86.3125
	150	0.0911	0.0421	128.2467
0.85	200	0.0788	0.0319	170.4290
	250	0.0706	0.0257	212.7465
	300	0.0644	0.0215	255.1412
	350	0.0597	0.0185	297.5806
	400	0.0558	0.0162	340.0457

While, for the truncated binomial and the truncated Poisson, the choice of the values for the parameters N and p to guarantee that the probability of the number of passengers onboard is less than, e.g., 10, is insignificant (i.e., close to zero), this is not the case with the truncated geometric. This is due to the choice of the geometric parameter required to guarantee a given mean. However, it is easy to modify this by ensuring that the mass of this geometric distribution has a positive value beyond a specific number, such as 10.

For the rate vector, $\boldsymbol{\theta_r}$, $1 \leq r \leq 6$, given the starting value, e.g., ϑ_1 (at 1), and the ending value, e.g., ϑ_N (at N), we consider four possible scenarios consisting of (a) linearly decreasing rates (LD); (b) quadratically decreasing rates (QD); (c) decreasing rates in a square root manner (SD); and (d) decreasing rates in a logarithmic manner (LG). Note that ϑ_1 and ϑ_N are, respectively, the rates when one passenger and N passengers are onboard. Naturally, we impose a restriction in which $\vartheta_1 > \vartheta_N$. Thus, we have the following.

LD: Here, we have (note that we suppress the suffix r in $\boldsymbol{\theta_r}$)

$$\theta_j = \vartheta_1 - \frac{\vartheta_1 - \vartheta_N}{N - 1}(j - 1), \ j = 1, \cdots, N. \tag{38}$$

QD: Here, we have

$$\theta_j = \vartheta_1 - \frac{\vartheta_1 - \vartheta_N}{(N - 1)^2}(j - 1)^2, \ j = 1, \cdots, N. \tag{39}$$

SD: Here, we have

$$\theta_j = \vartheta_1 - \frac{\vartheta_1 - \vartheta_N}{\sqrt{N - 1}}\sqrt{j - 1}, \ j = 1, \cdots, N. \tag{40}$$

LG: Here, we have

$$\theta_j = \vartheta_1 - \frac{\vartheta_1 - \vartheta_N}{log(N)}log(j), \ j = 1, \cdots, N. \tag{41}$$

Since the main goal of this work is to determine the impact of reducing the average boarding time on the other measures, we fix the average values of the times spent in various events, such as de-boarding, cleaning, boarding, and leaving a particular city for another city. In order to do this, we need to accordingly fix the means of the eight *PH*-distributions. To this end, we use Equation (16), which relates the means μ'_{W_i} to μ'_i, for $1 \leq i \leq 8$. Thus, given a specific probability vector p_r, the rate vector, θ_r, and the mean, μ'_{W_r}, we can find the value of μ'_r that will give the set value for μ'_{W_r}.

For the following two examples, we fix the input parameters as follows. The unit is the number of hours, unless otherwise indicated.

$$\mu'_{W_1} = \mu'_{W_2} = \mu'_{W_5} = \mu'_{W_6} = \frac{1}{3}, \mu'_{W_4} = \mu'_{W_8} = 2.$$

We take the probability vectors p_1 and p_2 to be identical, but we vary the common one to be one of the three, namely B, G, and P as listed above. Moreover, for the rate vectors, we take $\theta_1 = \theta_2 = \theta_4 = \theta_5$, and $\theta_3 = \theta_6$. The parameter values of $(\vartheta_1, \vartheta_N)$ for these two sets, namely for θ_1 and θ_3, will be $(12, 3)$ and $(12, 1.5)$. However, we vary the type of decreasing to be one of the four listed above. In Figure 1, we display a sample plot of the values of θ_j under the four scenarios: LD, QD, SD, and LG.
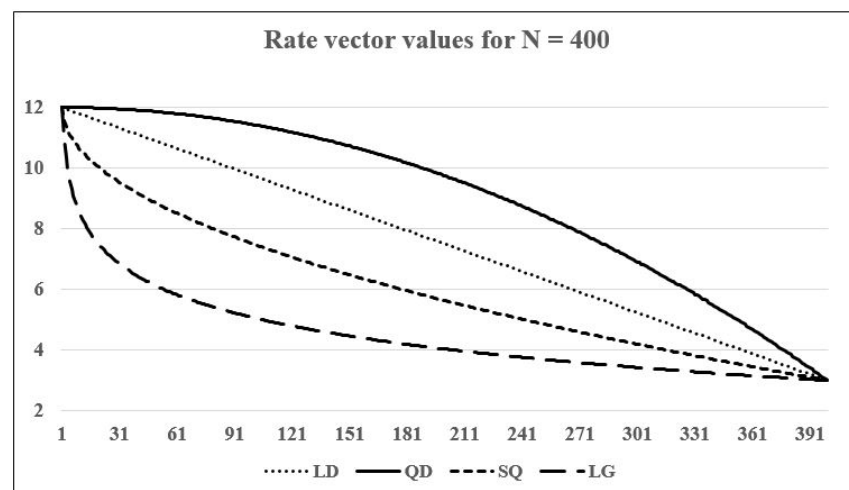
Figure 1. A sample plot of the rate vector under four scenarios.

The means, μ'_{W_3} and μ'_{W_7}, are varied from $\frac{25}{60}$ to $\frac{30}{60}$ in increments of 1 min, i.e., in increments of $\frac{1}{60}$ h. The capacity of the aircraft, N, is varied from 50 to 400 in increments of 50. To consider how, under the values chosen, the mean of the underlying random variable X_3 (and hence others), which can be controlled by the system providing the needed resources, behaves as we vary N, the type of probability vector, and the type of rate vector, we can consult the plots in Figures 2–4. Before we consider these (spider) figures, a few details are provided for explanation. The two-tuple values displayed at the perimeter of the outermost circle correspond to N and the mean times (in minutes). Thus, the two-tuple value 50 25 corresponds to $N = 50$ and the mean boarding time is 25 min. The legend containing B, G, and P indicates the type of distribution used to model the *PMF* of the number of passengers.
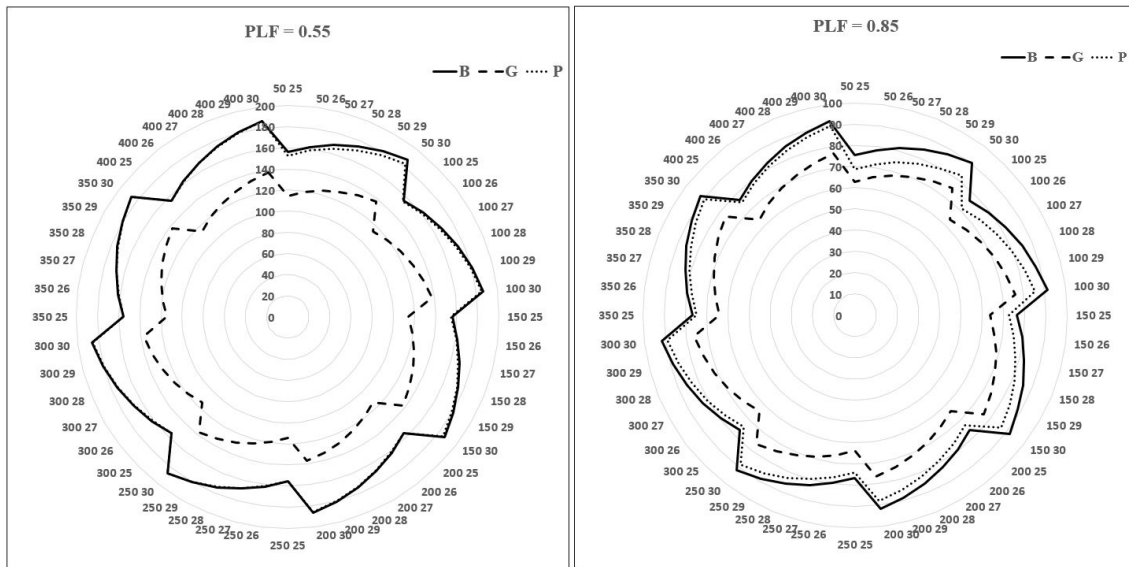
Figure 2. Plot of the mean of the boarding event with the *LD* rate under various scenarios.
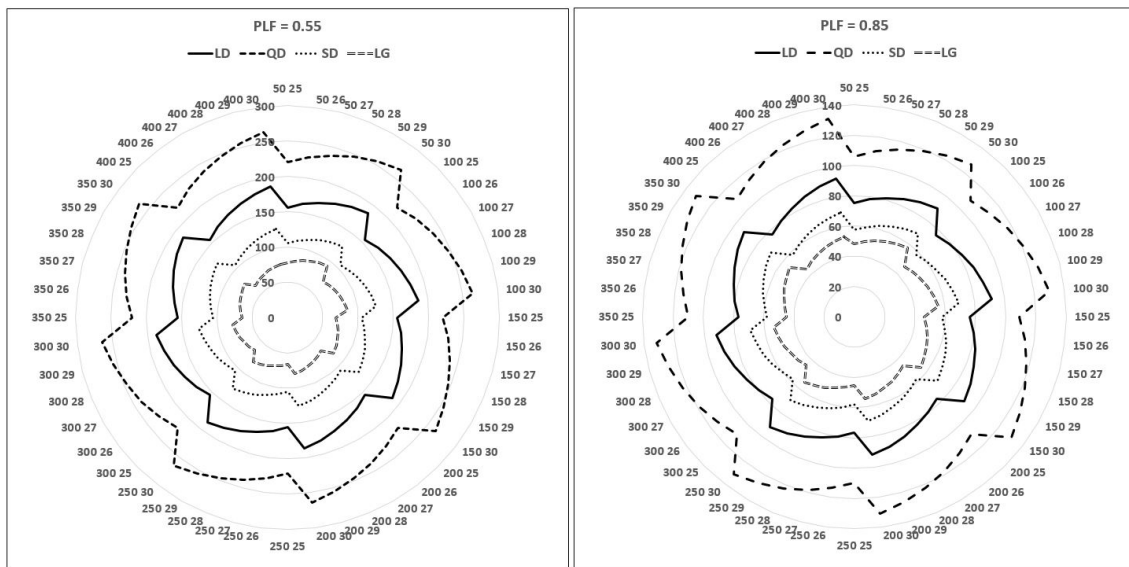

Figure 3. Plot of the mean of the boarding event using truncated binomial probabilities under various scenarios.

One can clearly notice the patterns in these plots, indicating significant changes to the mean as *N* and *PLF* are varied, as well as the type of probability vector (either truncated binomial or truncated geometric). However, we do not see a significant difference between the truncated binomial and truncated Poisson. As is to be expected, the mean increases as the average boarding time is increased under both values of *PLF* considered. This behavior indicates that an increase in the rate calls for additional resources or additional strategies to quicken the process of boarding. For example, this can be achieved by increasing the number of gate attendants (based on the value of *PLF*, which should be known ahead of time). Among the four types of rate vector considered, it appears that a quadratically decreasing rate gives the smallest mean (for X_3 and X_7), indicating that the system can dynamically provide gate attendants to help the passengers to board the aircraft.
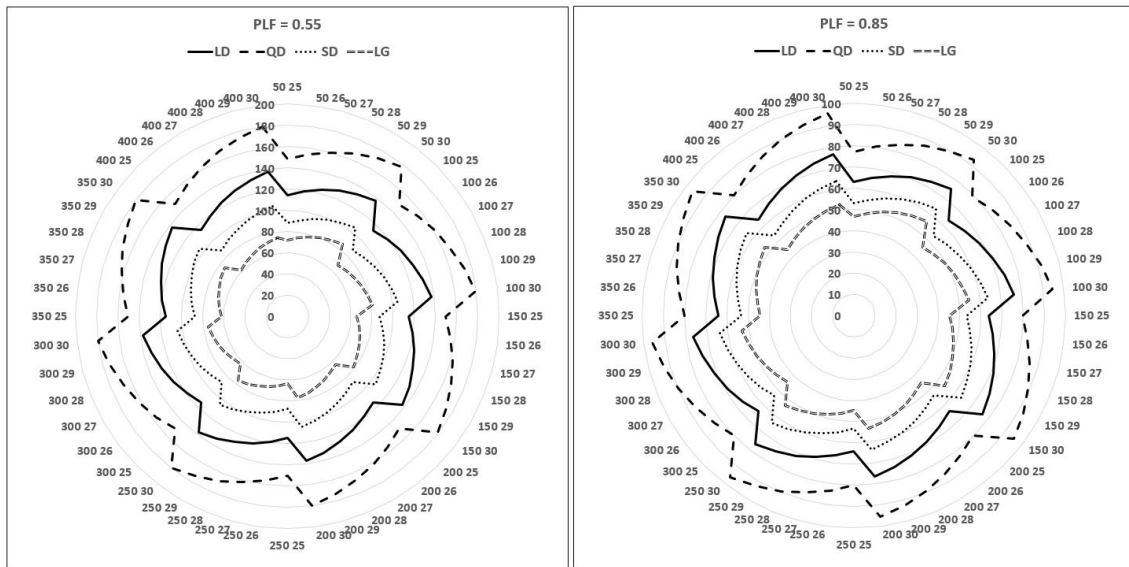
Figure 4. Plot of the mean of the boarding event using truncated geometric probabilities under various scenarios.

Illustrative Example 1: In this example, we use Erlang distributions for all underlying random variables. Recall that an Erlang of order m with parameter γ, denoted as $E(m, \gamma)$, has the *PDF* given by

$$f(t) = \frac{\gamma^m}{(m-1)!} t^{m-1} e^{-\gamma t}, \ t \geq 0. \tag{42}$$

Note that the mean and the variance are, respectively, given by $\frac{m}{\gamma}$ and $\frac{m}{\gamma^2}$. One advantage of using this probability function is that by choosing the order to be a large positive integer, we can model a random variable that has very minimal variation.

Using the notation $\mu_i = \frac{1}{\mu_i'}$, $1 \leq i \leq 8$, the order and the parameter values for this example are as follows.

$$X_1 \sim E(5, 5\mu_1), \ X_2 \sim E(50, 50\mu_2), \ X_3 \sim E(5, 5\mu_3), \ X_4 \sim E(100, 100\mu_4),$$
$$X_5 \sim E(5, 5\mu_5), \ X_6 \sim E(50, 50\mu_6), \ X_7 \sim E(5, 5\mu_7), \ X_8 \sim E(100, 100\mu_8). \tag{43}$$

The parameters N and $\mu_{W_3}' = \mu_{W_6}'$ are varied, respectively, from 50 to 400 and from 25 to 30 min in increments of 1 min. In Figures 5 and 6, respectively, we display the key measures for probability vectors labeled B and G under a linearly decreasing (LD) rate vector. Since we saw similar behavior for the other types of theta vectors, namely QD, SD, and LG, we display the results here only for the LD case.

It is clear by looking at these figures (as well as the ones not provided here due to the similarity of the plots) that the following occurs.

- Only the type of probability vector (whether it is truncated binomial or truncated geometric) and the type of theta vector (LD through LG) appear to have an impact on the percentiles.
- Comparing the truncated binomial probability (B) and the truncated geometric (G) schemes, we notice that (a) scheme G gives small values for the 50th percentile for both values of PLF; (b) for the 75th percentile, while scheme G gives small values when $PLF = 0.55$, the values are similar for both schemes when $PLF = 0.85$; (c) scheme B gives small values for the 95th percentile for both values of PLF. This indicates that

scheme *G* starts with small values for the percentiles (as compared to scheme *B*) and then yields progressively larger values for higher percentiles.
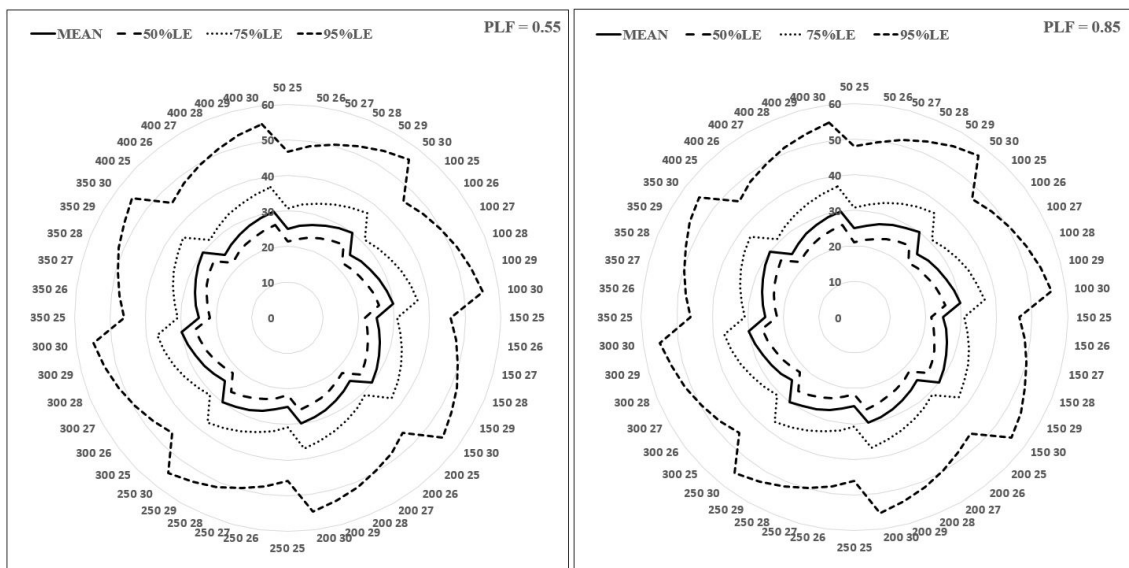

Figure 5. Plot of the measures of the boarding event with truncated binomial probabilities and *LD* rates under various scenarios.
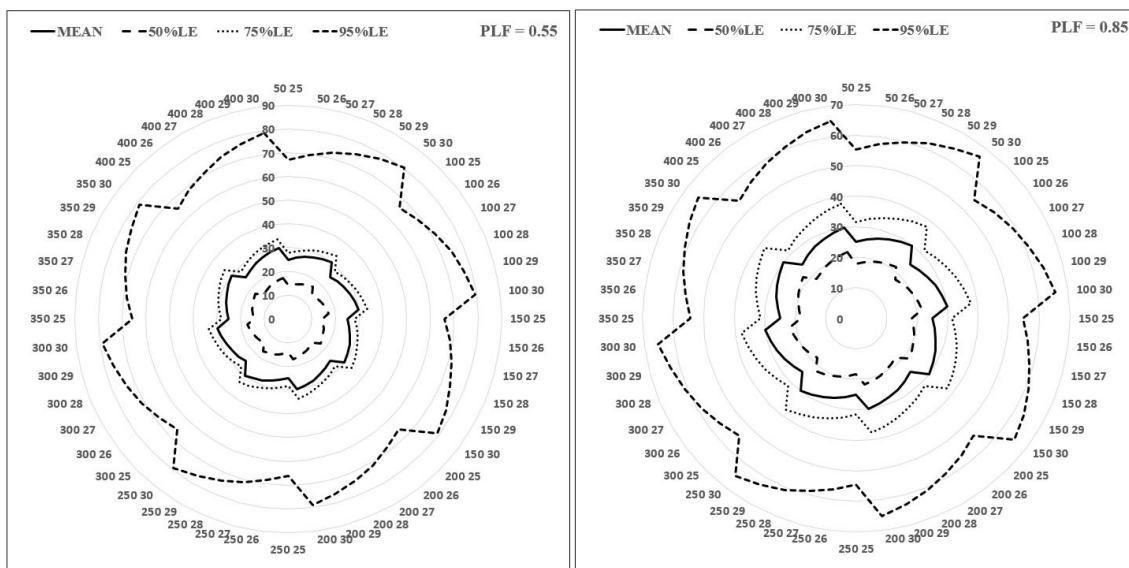

Figure 6. Plot of the measures of the boarding event with truncated geometric probabilities and *LD* rates under various scenarios.

Finally, we look at the percentage reduction in the percentiles when decreasing the average boarding time. We denote by $P_{(j)}^{(i)}$ the value of the *i*th percentile when the average boarding time is *j*. Thus, $P_{(25)}^{(50)}$ stands for the 50th percentile when the average boarding time is 25 min. The reduction percentage, for a given *i*th percentile and a given average boarding time *j*, is calculated as

$$100 \left[\frac{P_{(30)}^{(i)} - P_{(j)}^{(i)}}{P_{(30)}^{(i)}} \right]. \tag{44}$$

The reduction percentages do not appear to be significant when the probability vectors, the rate vectors, or *PLF* are changed. Hence, in Figure 7, we display the reduction percentages for the case of a truncated binomial and *LD* rate.
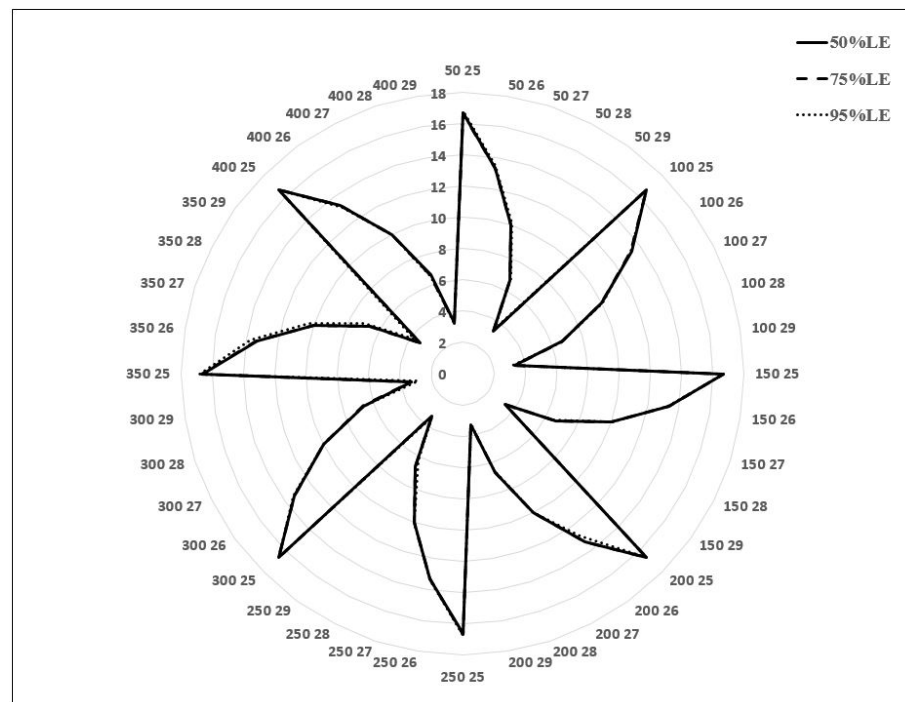
Figure 7. Plot of the reduction percentages for the percentiles under various scenarios.

It is very clear from this figure that the reduction percentages are almost identical for all three percentiles. Further, a 5 min reduction in the average boarding time results in a more than 16% reduction in the percentile value. This translates into a guarantee that, for at least 95% of the time, the boarding time will not exceed between 45 and 69 min depending on the value of *N*. The average 95% guarantee time across the board is about 50 min. If one were to give a guarantee at a 50% level, the boarding time will not exceed anywhere between 21 and 26 min depending on the value of *N*. The average 50% guarantee time across the board is about 25 min.

Illustrative Example 2: In this example, we use Erlang as well as hyperexponential distributions for the underlying random variables. Recall that a hyperexponential of order *m* with parameters $\gamma_1, \cdots, \gamma_m$, with the corresponding mixing probabilities, $q_1, \cdots, q_m$, has the *PDF* given by

$$f(t) = \sum_{k=1}^{m} q_j \gamma_j e^{-\gamma_j t}, \ t \geq 0. \tag{45}$$

Note that the mean and the variance are, respectively, given by $\sum_{k=1}^{m} \dfrac{q_k}{\gamma_k}$ and $2 \sum_{k=1}^{m} \dfrac{q_k}{\gamma_k^2} - \left(\sum_{k=1}^{m} \dfrac{q_k}{\gamma_k} \right)^2$. This probability function can be used when there is large variability in the underlying random variable. We will denote this hyperexponential by $HE\{(q_1, \cdots, q_m), (\gamma_1, \cdots, \gamma_m)\}$. The order and the parameter values for this example are as follows.

$$X_1 \sim E(5, 5\mu_1), \ X_2 \sim E(50, 50\mu_2),$$

$$X_3 \sim HE\{(0.50, 0.30, 0.15, 0.04, 0.01), \ \mu_3(10, 5, 2.5, 1.25, 0.625)\},$$

$$X_4 \sim E(100, 100\mu_4), \ X_5 \sim E(5, 5\mu_5), \ X_6 \sim E(50, 50\mu_6), \ X_8 \sim E(100, 100\mu_8),$$

$$X_7 \sim HE\{(0.50, 0.30, 0.15, 0.04, 0.01), \ \mu_7(10, 5, 2.5, 1.25, 0.625)\}.$$

As in the previous example, we vary the parameters N and $\mu'_{W_3} = \mu'_{W_6}$, respectively, from 50 to 400 and from 25 to 30 min in increments of 1 min.

In Figures 8 and 9, respectively, we display the key measures for probability vectors labeled B and G under a linearly decreasing (LD) rate vector.
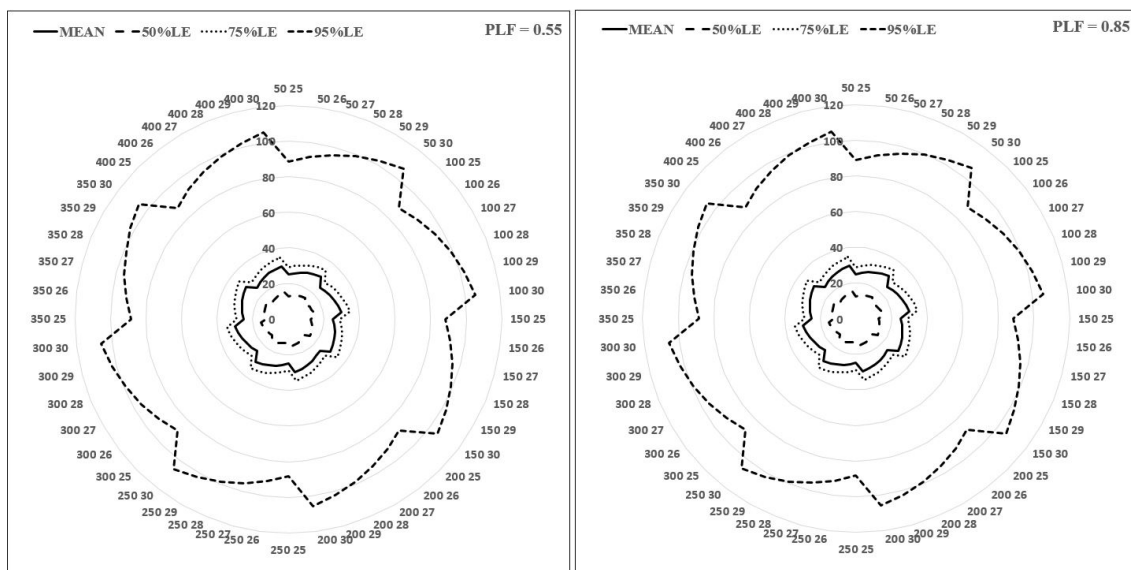
Figure 8. Plot of the measures of the boarding event with truncated binomial probabilities and LD rates under various scenarios.
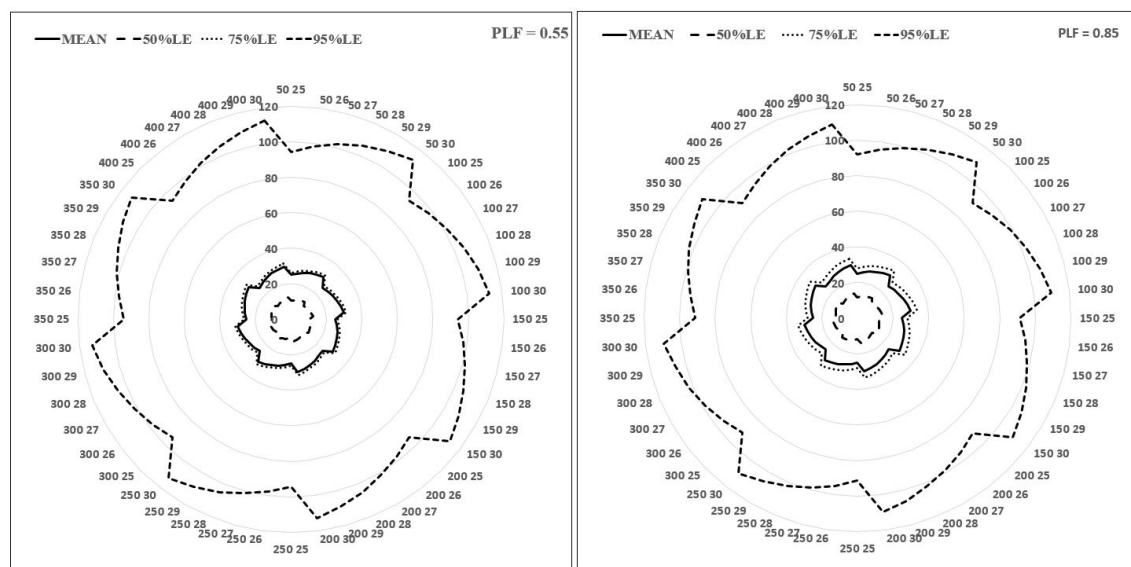
Figure 9. Plot of the measures of the boarding event with truncated geometric probabilities and LD rates under various scenarios.

It is clear by looking at these figures (as well as the ones not provided here due to the similarity of the plots) that the following occur.

- Only the type of probability vector (whether it is truncated binomial or truncated geometric) and the type of theta vector (*LD* through *LG*) appear to have an impact on the percentiles. This observation is similar to the one seen in the previous example.
- Comparing the truncated binomial probability (*B*) and the truncated geometric (*G*) schemes, we notice that (a) scheme *G* gives small values for the 50th percentile for both values of *PLF*; (b) for the 75th and the 95th percentiles, while scheme *G* gives small values when $PLF = 0.55$, the values are rather similar for both schemes when $PLF = 0.85$. This indicates that the large variability in the boarding times appears to nullify any significant differences in the *PLF* value, especially when the percentiles increase.

The plot of the reduction percentage for this example is almost identical to the one seen in the previous example and hence the figure is not displayed here. However, the guarantee times differ and the details are as follows. A 5 min reduction in the average boarding time results in a more than 16% reduction in the percentile value. This translates to a guarantee that, for at least 95% of the time, the boarding time will not exceed between 73 and 79 min depending on the value of *N*. The average 95% guarantee time across the board is about 75 min. If one were to provide a guarantee at a 50% level, then the boarding time will not exceed between 9 and 11 min depending on the value of *N*. The average 50% guarantee time across the board is about 10 min.

It is worth pointing out that, comparing the two illustrative examples, while the guarantee times at the 50% level are much smaller for the boarding times with large variability, at a 95% level, the guarantee times are small for the boarding times with small variability. This is probably due to the long tail of the probability distribution associated with the boarding time event.

Illustrative Example 3: Here, we provide a brief discussion of the *PDF* of the time to travel by looking at the case when $N = 200, PLF = 0.85$, with the truncated binomial probabilities and *LD* rates for the above-mentioned two illustrative examples. In Figure 10, we plot the representative *PDF* of the time to travel from city C_1 to city C_2 and then back to city C_1; moreover, the *PDF* of the travel time from city C_1 to city C_2 under three scenarios is plotted in Figure 11.
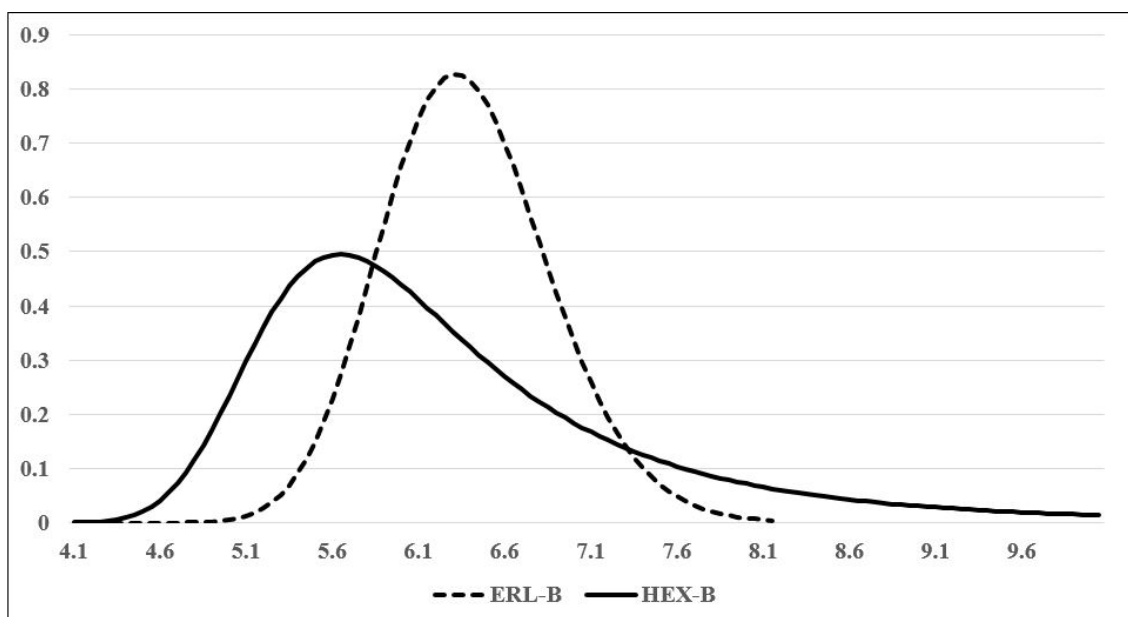

Figure 10. *PDF* of the travel time from city C_1 and back to city C_1.
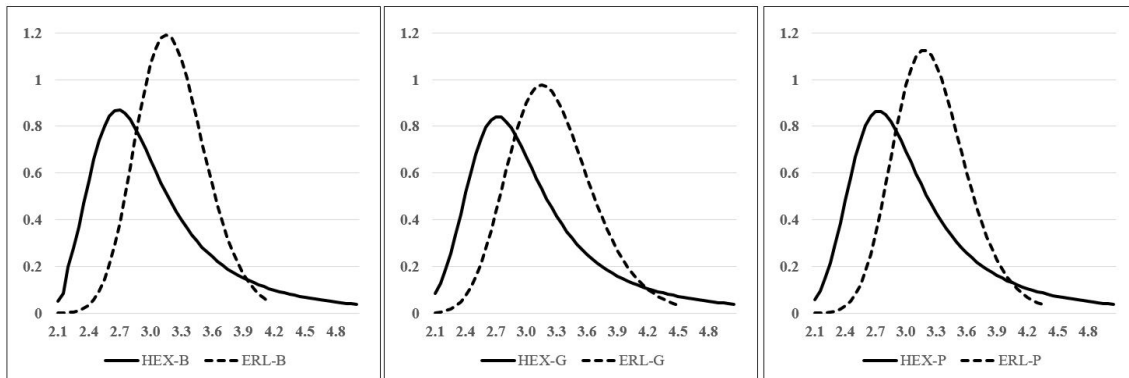
Figure 11. *PDF* of the travel time from city C_1 to city C_2.

It is evident from the above plots that, for all Erlang cases (see Illustrative Example 1), the *PDF* of the total travel time from city C_1 to city C_2 and back is a bell-shaped curve. Thus, one can try to fit a normal *PDF* with mean $\frac{19}{3}$ h and standard deviation 0.488975 h. For the *PDF* of the total travel time from city C_1 to city C_2 in the Erlang case (see Illustrative Example 1), the normal curves for the three schemes, *B*, *G*, and *P*, have the same mean of $\frac{19}{6}$ h but the standard deviations are, respectively, 0.343545 h, 0.430563 h, and 0.374347 h. This normal fit approximation will be helpful to managers seeking a quick solution using Excel or Excel-type worksheets in workplaces. Hence, we point out the possibility to implement the model proposed here.

In the case of Illustrative Example 2, wherein we used a hyperexponential distribution to model the boarding times, we notice a long-tailed distribution for the *PDF*. One can try to fit a three-parameter gamma, a three-parameter Weibull, or even a three-parameter log-normal distribution to approximate the *PDF* when dealing with a long-tailed distribution such as the one seen in the *PDF* plots. For example, we fitted a three-parameter gamma distribution with the shape, scale, and threshold parameters, respectively, of 29.0, 0.153, and 1.5 for the total travel time from city C_1 and back to city C_1.

5. Concluding Remarks

In this paper, we sought to address the boarding time, one of the major issues facing commercial airlines, using phase type distributions. While there is research on the study of boarding strategies that minimize the average boarding time, in this paper, our aim was to study the boarding time (as part of the process of traveling from one city to another) given a boarding strategy already in place. We used well-known probability distributions for the number of passengers boarding, as well as different schemes for the rates of processing of the passengers. We used the passenger load factor information from the Bureau of Labor Statistics [24]. However, there were no data available on the time to board, clean, or de-board or the actual flying time. Hence, we used hypothetical values based on personal experience in traveling, and this is a limitation of this model. However, when actual data are made available, one can use *PH* to fit the data and then apply the methodology suggested here. Through the qualitative analysis of the modeling of aircraft boarding, we found that a 5 min reduction in the average boarding time resulted in a more than 16% reduction in the values of the percentiles. This translates to a guarantee that, for at least 95% of the time, the boarding time will not exceed between 73 and 79 min depending on the value of the capacity of the aircraft. The average 95% guarantee time across the board is about 75 min. If one were to give a guarantee at a 50% level, then the boarding time will not exceed between 9 and 11 min depending on the value of of the capacity of the aircraft. The average 50% guarantee time across the board is about 10 min. Understanding the percentiles of the boarding times, as opposed to relying only on the average boarding times, will help management to adopt a better boarding strategy, which in turn will lead to an

increase in the number of trips that an aircraft can make. For example, when looking at the 95th percentile of the boarding time, there is a good understanding of how many trips an aircraft can make, as opposed to looking only at the average boarding time. Management can only incur a 5% error regarding the times in their estimations, as opposed to the error rate being unknown when using the mean, unless the boarding times are symmetric, in which case the error rate will be 50%. Thus, the use of percentiles to estimate and schedule the number of trips for an aircraft to make is more beneficial.

The model studied can be extended to include a variety of other aspects, such as (a) adding another random variable to model the time between the gate closing and the plane taking off (currently, we include this as part of the flying time); (b) the incorporation of catastrophic events (due to weather, a lack of aircraft personnel, or the mechanical failure of the aircraft), leading to the cancellation of a flight from a particular city; (c) extending from two cities to more than two cities; and (d) using practical data to fit the probability function for (i) the number of passengers boarding; (ii) the time to clean the aircraft; and (iii) the time taken from the moment that the gate closes to the aircraft's landing in another city. Another task of interest for future work is to compare different boarding processes and identify which one will contribute to reducing the boarding times; then, this boarding process can be used in the model studied here to estimate the increase in the average number of trips that can be made.

Data Availability Statement: No new data were created or analyzed in this study.

Conflicts of Interest: The author declares no conflicts of interest.

References

1. Available online: https://www.wsj.com/articles/southwest-airlines-boarding-seating-turn-ee12d3f2 (accessed on 1 June 2024).
2. Yeager, M. What Does It Take to Get a Plane Ready Between Flights? Americal Airlines Shows Us. *The Arizona Repulbic*, 14 May 2019.
3. Available online: https://www.nytimes.com/2011/11/01/business/airlines-are-trying-to-cut-boarding-times-on-planes.html (accessed on 1 June 2024).
4. Bachmat, E.; Berend, D.; Sapir, L.; Skiena, S.; Stolyarov, N. Analysis of Airplane Boarding Times. *Oper. Res.* **2009**, *57*, 499–513. [CrossRef]
5. Bachmat, E.; Khachaturov, V.; Kuperman, R. Optimal back-to-front airplane boarding. *Phys. Rev. E* **2013**, *87*, 062805. [CrossRef] [PubMed]
6. Bachmat, E. Airplane boarding, disk scheduling, and Lorentzian geometry. In *Mathematical Adventures in Performance Analysis: From Storage Systems, through Airplane Boarding, to Express Line Queues*; Springer International Publishing: Cham, Swizterland, 2014; pp. 51–129. [CrossRef]
7. Erland, S.; Bachmat, E.; Steiner, A. Let the fast passengers wait: Boarding an airplane takes shorter time when passengers with the most bin luggage enter first. *Eur. J. Oper. Res.* **2022**, *317*, 748–761. [CrossRef]
8. Hutter, L.; Jaehn, F.; Neumann, S. Influencing factors on airplane boarding times. *Omega* **2019**, *87*, 177–190. [CrossRef]
9. Available online: https://simpleflying.com/fastest-boarding-type-guide/ (accessed on 1 June 2024).
10. Available online: https://www.azcentral.com/story/travel/airlines/2019/05/14/how-long-it-takes-to-get-a-plane-ready-between-flights-airplane-turnaround-time/1123694001/ (accessed on 1 June 2024).
11. Available online: https://www.skyparksecure.com/blog/fastest-plane-boarding-methods/ (accessed on 1 June 2024).
12. Steffen, J. Optimal boarding method for airline passengers. *J. Air Transp. Manag.* **2008**, *14*, 146–150. [CrossRef]
13. Available online: https://www.usatoday.com/story/travel/columnist/hobica/2017/11/21/airline-boarding-order/881548001/ (accessed on 1 June 2024).
14. Willamowski, F.; Tillmann, A.M. Minimizing Airplane Boarding Time. *Transp. Sci.* **2022**, *56*, 1196–1218. [CrossRef]
15. Neuts, M.F. Probability distributions of phase type. In *Liber Amicorum Prof. Emeritus H. Florin*; Department of Mathematics, University of Louvain: Ottignies-Louvain-la-Neuve, Belgium, 1975; pp. 173–206.
16. Bladt, M.; Nielsen, B.F. *Matrix-Exponential Distributions in Applied Probability*; Probability Theory and Stochastic Modelling; Springer: Boston, MA, USA, 2017; Volume 81.
17. Buchholz, P.; Kriege, J.; Felko, I. *Input Modeling with Phase-Type Distributions and Markov Models: Theory and Applications*; Springer: Heidelberg, Germany, 2014.
18. Chakravarthy, S.R. *Introduction to Matrix-Analytic Methods in Queues*; John Wiley & Sons, Inc.: London, UK, 2022; Volume 1.
19. Latouche, G.; Ramaswami, V. *Introduction to Matrix Analytic Methods in Stochastic Modeling*; SIAM: Philadelphia, PA, USA, 1999.

20. Neuts, M.F. *Matrix-Geometric Solutions in Stochastic Models: An Algorithmic Approach*; John Hopkins University Press: Baltimore, MD, USA, 1981.
21. Graham, A. *Kronecker Products and Matrix Calculus with Applications*; Ellis Horwood: Chichester, UK, 1981.
22. Marcus, M.; Minc, H. *A Survey of Matrix Theory and Matrix Inequalities*; Allyn and Bacon: Boston, MA, USA, 1964.
23. Steeb, W.H.; Hardy, Y. *Matrix Calculus and Kronecker Product*; World Scientific Publishing: Singapore, 2011.
24. Available online: https://www.transtats.bts.gov/Data_Elements.aspx?Data=1 (accessed on 15 March 2023).
25. Asmussen, S.; Nerman, O.; Olsson, M. Fitting phase-type distributions via the EM algorithm. *Scand. J. Stat.* **1996**, *23*, 419–441.
26. Bobbio, A.; Cumani, A. ML estimation of the parameters of a PH distribution in triangular canonical form. In Proceedings of the 5th International Conference on Modelling Techniques and Tools for Computer Performance Evaluation (TOOLS), Torino, Italy, 13–15 February 1991.
27. Bobbio, A.; Telek, M. A benchmark for PH estimation algorithms: Results for acyclic-PH. *Commun. Stat. Stoch. Model.* **1994**, *10*, 661–677. [CrossRef]
28. Esparza, L.J.R. Maximum Likelihood Estimation of Phase-Type Distributions. Ph.D. Dissertation, Technical University of Denmark, Kongens Lyngby, Denmark, 2011.
29. Feldmann, A.; Whitt, W. Fitting mixtures of exponentials to long-tail distributions to analyze network performance models. *Perform. Eval.* **1998**, *31*, 245–279. [CrossRef]
30. Okamura, H.; Dohi, T. Fitting phase-type distributions and Markovian arrival processes: Algorithms and tools. In *Principles of Performance and Reliability Modeling and Evaluation: Essays in Honor of Kishor Trivedi on his 70th Birthday*; Springer: Heidelberg, Germany, April 2016.
31. Reinecke, P.; Krauss, T.; Wolter, K. Cluster-based fitting of phase-type distributions to empirical data. *Comput. Math. Appl.* **2012**, *64*, 3840–3851. [CrossRef]
32. Thummler, A.; Buchholz, P.; Telek, M. A novel approach for phase-type fitting with the EM algorithm. *IEEE Trans. Depend. Secur.* **2006**, *3*, 245–258. [CrossRef]